Published in final edited form as:
J Am Chem Soc. 2009 September 16; 131(36): 12960–12969. doi:10.1021/ja9016864.

Enhanced Photostability of Genetically Encodable Fluoromodules Based on Fluorogenic Cyanine Dyes and a Promiscuous Protein Partner

Nathaniel I. Shank[1], **Kimberly J. Zanotti**[1], **Frederick Lanni**[2,3], **Peter B. Berget**[2,3], and **Bruce A. Armitage**[1,3,*]

[1] Department of Chemistry, Carnegie Mellon University, 4400 Fifth Avenue, Pittsburgh, PA 15213

[2] Department of Biological Sciences, Carnegie Mellon University, 4400 Fifth Avenue, Pittsburgh, PA 15213

[3] Department of Molecular Biosensor and Imaging Center, Carnegie Mellon University, 4400 Fifth Avenue, Pittsburgh, PA 15213

Abstract

Fluoromodules are discrete complexes of biomolecules and fluorogenic dyes. Binding of the dyes to their cognate biomolecule partners results in enhanced dye fluorescence. We exploited a previously reported promiscuous binding interaction between a single chain, variable fragment antibody protein and a family of cyanine dyes to create new protein-dye fluoromodules that exhibit enhanced photostability while retaining high affinity protein-dye binding. Modifications to the dye structure included electron withdrawing groups that provide resistance to photo-oxidative damage. Low nanomolar equilibrium dissociation constants were found for the new dyes. Fluorescence microscopy illustrates how yeast can be surface-labeled with three different colors based on a single protein and appropriately chosen dyes.

INTRODUCTION

The development of fluorescent proteins such as GFP[1,2] has revolutionized bioimaging due to the ability to make genetically encoded fusion constructs in which the fluorescent protein is tagged to a protein of interest.[3–6] However, it is difficult to precisely tune properties such as color, quantum yield and photostability of these proteins because the fluorophore is an integral part of the protein structure. We recently developed an alternative technology based on single chain variable fragment (scFv) antibodies and noncovalently bound fluorogenic dyes.[7] The protein component, known as a fluorescence-activating protein or FAP, binds with high affinity to the dye, leading to 10^2–10^3-fold enhancement of the dye fluorescence. We refer to the dye-protein pair as a fluoromodule; recent efforts from our Center have yielded a catalogue of fluoromodules that span much of the visible and near-IR regions of the spectrum.[8] The FAPs can be genetically encoded as fusion constructs in the same way as inherently fluorescent proteins such as GFP. Provided the fluorogenic dye can be delivered to the site where the FAP is expressed, the fluoromodule will be reconstituted, resulting in fluorescence only at that site. Fluorescence can be observed immediately after folding of the protein, provided the dye is

*Tel: 412-268-4196; Fax: 412-268-1061; army@cmu.edu.

Supporting information available: Fluorescence K_d determination for α-CN-DIR with yeast cell surface-displayed K7, UV-vis absorbance spectra of TO and fluorinated analogues bound to K7, and merged fluorescence and DIC micrographs of K7-expressing yeast stained with TO-4F, α-CN-DIR and DIR.

already present. This is in contrast to the significant maturation time required to form the GFP fluorophore after folding of the protein. Moreover, our technology will also allow for on-demand applications, where fluorescence is desired only at a specific time determined by when the dye is added.

Our fluoromodule development method relies on (1) design and synthesis of fluorogenic dyes and (2) selection of cognate FAPs from a yeast surface-displayed scFv library. Having the library displayed on yeast allows flow cytometry to be used for FAP selection, providing an efficient and powerful approach to obtaining high affinity and high quantum yield fluoromodules. Our initial report demonstrated selection, characterization and imaging applications of scFv-based fluoromodules that utilized the fluorogenic dyes malachite green and thiazole orange.[7] A second paper described fluoromodules based on a new cyanine dye known as dimethylindole red (DIR).[8,9] We were intrigued by the fact that one of the proteins selected for DIR exhibited considerable promiscuity, binding to several other cyanine dyes with low nanomolar affinities, providing fluorescence across much of the visible and near-IR regions of the spectrum. In this report, we take advantage of the permissive binding behavior of this protein to create new fluoromodules that exhibit improved photostability due to rational modifications to the fluorogenic dye structures. Specifically, introduction of electron-withdrawing cyano and fluoro substituents to the cyanine dye bridge and heterocycles in order to suppress oxidative photobleaching of the dye leads to significantly enhanced photostability of the corresponding fluoromodules without significantly compromising the dye-protein binding affinity.

RESULTS

The fluorogenic dyes used for these experiments are shown in Chart 1. These dyes were chosen for analysis based on their structural similarity to DIR and TO, and contained modifications that were expected to increase photostability. With regards to fluorination, Renikuntla et al[10] and Silva et al[11] previously showed that polyfluorination of benzothiazole-containing cyanines led to marked increases in photostability compared to the parent dyes. Similar results have been observed for fluorinated versions of the commonly used dye fluorescein[12], its biarsenical analogue "FlAsH"[13] and coumarins[14]. The precedent for incorporating a cyano group in the methine bridge came from the work of Toutchkine et al, where two cyano functionalized merocyanine dyes showed improved photostability over the unfunctionalized derivative.[15] These earlier reports attribute the increased stability to the electron withdrawing ability of the substituent(s), which should make the dyes less reactive toward singlet oxygen generated during irradiation. It is also possible that the fluorinated dyes generate singlet oxygen less efficiently, although this has not been determined.

The syntheses of DIR and the fluorinated TO dyes were reported previously.[9,11] Synthesis of the α-CN DIR analogue is shown in Scheme 1. Commercially available 1,3,3-trimethyl-2-methyleneindole (**1**) was converted to the corresponding nitrile (**2**) in two steps as described by Toutchkine.[15] A Vilsmeier-Haack reaction was used to introduce an aldehyde on the alpha carbon (**3**).[16] Intermediate **3** was then reacted with alkylated lepidine (**4**) to produce the dye in adequate yield.

DIR versus α-CN-DIR

The methine bridge-substituted dye α-CN-DIR is a green solid which gives bright pink solutions having a maximum absorption at 526 nm in aqueous phosphate buffer (Figure 1A). This corresponds to an 82 nm blue-shift in absorption relative to unsubstituted DIR (λ_{max} = 610 nm); a similar hypsochromic effect of a cyano group was also observed for merocyanine dyes.[15]

The absorption maximum and molar absorptivity for α-CN-DIR are unchanged in the presence of the K7 protein, but a slight red-shift and decrease in absorptivity are observed in a 90% glycerol-in-water solution. The fluorogenicity of the new dye is evident in the >20-fold increase in fluorescence observed in the viscous solvent, relative to aqueous buffer (Figure 1B). The dye exhibits a similar enhancement of fluorescence in the presence of the K7 scFv, demonstrating that the new dye still binds to the scFv originally selected for binding to the unsubstituted parent dye DIR. Interestingly, the emission spectrum also shifts by 25 nm to the blue when bound to the protein versus solvated in glycerol. In contrast, DIR only shows a 9 nm blue shift (650 nm in glycerol, 641 nm bound to K7), suggesting a greater sensitivity to solvent polarity for the α-CN analogue.

We next determined the dissociation constant for α-CN-DIR with K7 by fluorescence titration (Figures 2 and S1). Relative to DIR, the K_d value was approximately 6-fold higher (63.3 ± 3.8 nM) for K7 in solution and 3-fold higher (41.9 ± 1.9 nM) for K7 displayed on the yeast cell-surface (Table 1). We also measured fluorescence quantum yields for the dyes in glycerol and K7 (Table 1). DIR and α-CN-DIR exhibit similar quantum yields in glycerol, but K7 more strongly enhances the fluorescence of DIR. The weaker binding to protein and lower quantum yield of αCN-DIR indicates that the cyano group perturbs interactions that lead to dye-protein recognition. High-resolution structural information will help to determine whether this is due to a direct steric clash between the cyano group and the protein or to an indirect electronic effect, as observed for a stilbene-binding scFv reported previously.[17]

Photobleaching of DIR and α-CN-DIR was carried out in 90% glycerol or in the presence of K7 as described in the Experimental section. Both dyes demonstrate better photostability when bound to the protein compared with being dissolved in the viscous solvent, indicating a protective effect of the protein matrix (Figure 3). As expected, α-CN-DIR exhibited superior photostability, requiring 6–7-fold longer irradiation to produce comparable loss of fluorescence intensity compared with DIR. Thus, the slightly lower affinity and fluorescence quantum yield for α-CN-DIR bound to K7 are compensated by a significantly greater photostability.

Photobleaching of cyanine dyes is attributable at least in part to singlet oxygen produced in situ by the relatively small fraction of the dye excited state that intersystem crosses to the triplet, which then undergoes energy transfer to ground state oxygen:

$$^1\mathrm{Dye}^* + {}^3\mathrm{O}_2 \rightarrow {}^3\mathrm{Dye}^* + {}^3\mathrm{O}_2 \rightarrow {}^1\mathrm{Dye} + {}^1\mathrm{O}_2{}^*$$

Our rationale for incorporating the cyano group at the alpha carbon of DIR was to reduce the dye's reactivity toward singlet oxygen.[15] To test this hypothesis, we used sodium molybdate, which reacts under basic conditions with hydrogen peroxide to generate singlet oxygen via a thermal process.[18–20] (K7 binding and fluorescence enhancement of the cyanines were unaffected by the basic pH required for this reaction.) We first tested the reactivity of the dyes in the absence of K7 protein, necessitating analysis by absorbance rather than fluorescence. As shown in Figure 4, DIR underwent 42% loss of absorbance after 40 min reaction. We repeated the experiment in the presence of 90% D_2O, which increases the lifetime of singlet oxygen.[21] We observed an increase in bleaching to 74%, verifying the involvement of singlet oxygen in the reaction (Figure 4B). In contrast, α-CN-DIR bleached only 8% in H_2O, consistent with a stabilizing effect of the α-CN modification by reducing reactivity toward singlet oxygen.[15]

We next repeated the experiment in the presence of K7 (Figure 5). Interestingly, DIR exhibited significantly reduced bleaching during the experiment (20% vs 42% in the absence of K7, Figure 4). This result indicates that the dye is significantly protected from oxidative damage

by binding to the protein. This could be due to steric blockage by the protein or to quenching of the singlet oxygen by the protein.[22] The protecting effect of the protein was also evident in the direct photobleaching experiments shown in Figure 3, where the protein-bound dyes bleached slower than dyes dissolved in glycerol. Interestingly, D_2O failed to increase the bleaching yield of protein-bound DIR, in contrast to the reaction of free dye shown in Figure 4B.

It is important to note that, even though DIR photobleaches considerably faster than αCN-DIR (Figure 3), DIR fluoromodules can be regenerated after photobleaching, provided the bleached dye can dissociate from the protein and be replaced by a pristine dye from the solution. This feature is demonstrated in Figure 6, where irradiation of a 1:1 mixture of DIR/K7 at 250 nM, i.e. 25 times the K_d, leads to 55 (±7) % loss of DIR fluorescence. Subsequent addition of another equivalent of DIR restores most of the fluorescence (89% of the original value), while addition of a second equivalent of fresh DIR has no further effect (data not shown). This result indicates that the damage that causes photobleaching is primarily localized to the dye rather than to the protein and that the bleached DIR is readily displaced from the protein by undamaged dye. The failure to completely recover the starting fluorescence could be due to a minor amount of damage to the protein rather than to the dye or to covalent linkage between the bleached dye and the protein. Further experiments will be required to resolve this question.

When we repeated the experiment shown in Figure 6 using 90% D_2O, no significant change in bleaching was observed (55% for H_2O vs 57% for D_2O). This result indicates that photobleaching of the protein-bound dye does not involve *diffusible* singlet oxygen and is consistent with Figure 5, where D_2O failed to enhance molybdate-peroxide induced bleaching of K7-bound DIR. Of course, this does not rule out a mechanism where singlet oxygen generated by the protein-bound dye reacts rapidly with the dye before diffusing into the surrounding medium.

TO versus Fluorinated Analogues

We next characterized the effect of ring fluorination on a thiazole orange-based fluoromodule. Initial experiments were conducted to determine whether the dyes were fluorogenically activated by yeast-surfaced displayed K7. Equilibrium binding constants for the dye-scFv interactions were calculated by titrating dye into a culture of yeast-surface displayed K7 and measuring the resulting fluorescence. Control experiments were also conducted where dye was titrated either into yeast that did not express K7 or into aqueous buffer. Figure 7 shows the titration of TO into K7, which yielded K_d = 119 nM. Although the data are well fit by a 1:1 binding model, a substantial background fluorescence signal was seen for TO and the fluorinated derivatives in the presence of yeast that did not express K7. This is in contrast to our prior work with DIR, for which there was virtually no background. The high background fluorescence for yeast that were not induced to express K7 is likely due to the presence of dead cells (ca. 0.5–1.0% of the total cell population, on average), which have compromised membranes. Dye molecules can enter into dead cells and intercalate into DNA, resulting in fluorescence enhancement. DIR was designed to prevent intercalation by virtue of its bulky dimethylindole ring and negatively charged sulfonate group.[9] However, TO possesses neither of these structural features and can therefore bind to DNA, presumably by intercalation,[11] leading to the significant fluorescence signal seen in the control sample. This hypothesis was tested using confocal fluorescence microscopy (Figure 7, right), where yeast that express K7 on their surface show the expected halo of green fluorescence, whereas yeast that do not express K7 show only a single bright cell that exhibits uniform fluorescence throughout. Based on these results, all other experiments were performed using purified soluble K7 protein rather than yeast-displayed K7.

Dissociation constants for the soluble K7-TO pairs were measured by fluorescence titration (Figure 8 and Table 1). The TO dyes bind at least as tightly as DIR, even though K7 was originally selected for binding to the longer trimethine dye. The lone exception is TO-CF_3, in which the larger trifluoromethyl group slightly weakens the binding, similar to the cyano group in α-CN-DIR.

The soluble protein exhibited several-fold tighter binding compared to the yeast surface-displayed scFv for dyes with a fluorinated benzothiazole ring, while only a slight change in K_d occurred upon addition of a trifluoromethyl group to the quinoline ring. The smaller dissociation constants suggest that the dyes are held more rigidly by the purified K7 protein, preventing the relaxation of the excited state through vibronic pathways.[11] This explanation gains further support when the fluorescence spectra of the yeast surface-displayed and soluble K7-dye pairs are compared (Figure 9). Broader peaks are clearly present in the yeast surface-displayed samples, indicative of the dyes having greater torsional flexibility compared to the narrower spectra of dye-scFv that also show a vibronic shoulder, consistent with decreased dye mobility within the binding pocket, although broadening of the spectra could also be due to binding to other sites, such as the yeast surface or to DNA in dead cells. The apparently weaker binding to the yeast surface-displayed version of the protein could be due to misfolding of the protein, competitive binding of the dye to the cell membrane instead of the protein, or to perturbation of the fluorescent signal by dead cells, where the dye can intercalate into cellular nucleic acids.

Absorbance spectra of the soluble K7-TO dye pairs were collected (Supporting information, Figure S2). As observed previously for these dyes in solution and when bound to DNA,[11] fluorination of the benzothiazole ring system leads to blue-shifted absorption spectra whereas introduction of the trifluoromethyl group to the quinoline heterocycle results in a red-shift.

The fluorescence quantum yields for the TO dyes were also determined (Table 1). The quantum yields in the presence of soluble K7 compared favorably to the quantum yields in 90% glycerol with the protein-bound dyes being consistently brighter than the dyes in glycerol (up to 8-fold for TO-2pF and TO-CF_3). The observed trend in glycerol is for the quantum yield to increase as the electron-withdrawing character of the benzothiazole heterocycle increases, while adding the electron-withdrawing CF_3 group to the quinoline heterocycle causes a decrease in φ_f. This trend is reproduced when the dyes are bound to K7, with the exception of TO-4F, which exhibits a lower φ_f than TO-2pF. Note that the quantum yields were measured at concentrations well above the K_d.

The photostability of the dye-scFv fluoromodules was also determined (Figure 10). The tetrafluorinated dye TO-4F exhibited greater photostability than the other dyes (ca. 4-fold more stable than the unsubstituted TO), in agreement with previously published data measuring the photostability of these dyes in either aqueous buffer or calf thymus DNA.[11] The addition of highly electron-withdrawing substituents such as fluorine should create a more positive oxidation potential, resulting in substantially increased photostability.[10]

Fluorescence Imaging

We next tested the new dyes for imaging of cell-surface expressed K7. Figure 11 shows images acquired after staining of K7-expressing yeast with TO-4F (green), α-CN-DIR (orange) and DIR (red), illustrating the tunable emission color available by using different dyes with this single protein. Note that these images were acquired without washing away unbound dye, demonstrating the value of using fluorogenic dyes in this technology: the low fluorescence quantum yield of the unbound dye provides excellent contrast in the images.

DISCUSSION

GFP is one of the most commonly used fluorescent cellular tags. Although GFP mutants that exhibit new colors and can be used to detect environmental changes have been identified,[23] the relatively slow maturation time required to produce the fluorophore in GFP makes it difficult to track a protein during the early, post-translational period. The scFv-dye fluorescence of our fluoromodules can be visualized almost immediately after protein folding because dye binding will be limited primarily by diffusion. Moreover, because the dye is nonfluorescent until binding to the scFv, an excess of dye can be used to further increase the rate of fluoromodule reconstitution without introducing significant background fluorescence, provided the dye is properly designed to avoid binding to cellular components such as genomic DNA, as we reported previously for DIR.[9]

While natural fluorescent proteins require integral fluorophores, several other technologies besides our fluoromodules have been developed that rely on exogenous dyes. For example, incorporation of tetracysteine or hexahistidine motifs into proteins allows capture of biarsenical[24] or divalent metal ion-ligated[25] dyes respectively. However, the high toxicity of the biarsenical dyes requires the addition of antidotes (e.g. 1,2-thiols or phosphines). Hauser et al recently improved upon the hexahistidine label by synthesizing a dye that utilizes Zn^{2+} instead of Ni^{2+} as the multi-dentate metal center involved in binding, greatly decreasing the system's toxicity. The biarsenical fluorescein derivative "FlAsH" exhibits a larger fluorescence enhancement upon binding than the scFv-dye pairs, although the scFv-enhanced dye fluorescence is typically >100-fold and the color selection is considerably broader.

Phage displayed peptide or protein libraries provide an alternate method for selecting high affinity binders to a target molecule. This approach has been successfully used to generate "fluorettes," in which a small peptide is selected based on its ability to bind to fluorescent dyes such as Texas Red or the structurally similar calcium sensor X-rhod.[26,27] However, as is often observed for peptides derived from phage display, binding was lost for soluble versions of some peptides. This indicates that, in these cases, the multivalent display format used for selection is needed to maintain high affinity binding in the absence of the phage surface. It is unclear if relatively small, monovalent peptides will contain sufficient binding determinants to provide high affinity and selectivity for fluorogenic dyes such as those used in our fluoromodules.

Another technology that is related to our work involves fluorescent dyes that are conjugated to a quencher group.[28] In aqueous solution, the unbound hapten stacks with the fluorophore to quench its fluorescence, resulting in a low background fluorescence signal. Fluorescence is restored in the presence of an scFv that binds specifically to the quencher group. (A similar approach has been used recently to create RNA-based fluoromodules.[29,30]) This system has been employed *in vivo* to monitor pH changes in Golgi. With this technology, a variety of dye colors can be created by attaching the universal quencher group to a desired fluorophore. While this versatility is appealing in terms of using the same scFv for any color, the fact that the scFv-quencher interaction is the same for all cases precludes multicolor experiments, until additional scFv-quencher pairs are developed.

Our fluoromodule system is similar to the hapten fluorophore conjugates in that dye fluorescence is enhanced upon binding to an scFv. However, dyes such as DIR and TO are inherently nonfluorescent. No hapten attachment is required to quench the dye signal, allowing for the use of smaller dye molecules. By using an antibody library, we are also able to select different scFvs that bind selectively to different dyes,[7,8] whereas the hapten fluorophores only use a single scFv to bind to the hapten half of the target molecule. Difficulties are present when attempting multicolor labeling with the hapten fluorophores, because a single scFv binds to all

of the hapten-dye conjugates. By contrast, although K7 is promiscuous, multiple other scFv-dye pairs selected by our antibody library screening method can be used simultaneously, allowing for multicolor labeling across the spectrum.[7]

A problem shared by both our fluoromodule system and the quencher-fluorophore conjugates is the need to form disulfide bonds among integral cysteines in the scFvs. In the reducing environment of the cytoplasm, difficulty in forming disulfides could lead to misfolding of the protein and impaired fluorogen binding. Current work is underway in our labs to replace the cysteines with other amino acids, and then use affinity maturation to regain any loss of dye binding or fluorescence enhancement.

As demonstrated by Özhalici-Ünal et al[8] and again here, the scFv K7 is capable of binding a structurally diverse set of cyanine dyes whose emission wavelengths span most of the visible and near-IR spectrum. Numerous modifications of the dye heterocycles, substituents and polymethine bridge are tolerated by K7 without significant loss of affinity. While a detailed understanding of the protein's promiscuity awaits a high-resolution structure and/or mutagenesis studies, our current knowledge allows dyes (and colors) to be chosen based on laser and filter set availability as well as general experimental design. The dyes used in the current study featured structural modifications that were expected to impart enhanced photostability to the fluoromodules. Thus, the promiscuity of the K7 protein allows fine-tuning of the dye properties without having to select new FAPs from the naïve yeast-displayed library. However, if even higher affinity were desired for a given K7-dye combination, an affinity maturation process consisting of randomly mutagenizing the K7 gene and re-selecting for binding of dye at dye concentrations below the K_d of the wild-type protein can lead to substantially tighter binders.[7] In addition, the α-CN-DIR/K7 pair fluoresces in a wavelength region that was not covered in our original report.

Our fluoromodules exhibit one additional advantage over inherently fluorescent proteins such as GFP and other labeling technologies. In the case of GFP, no means exists to replenish the signal lost when the chromophore is photobleached since the chromophore is covalently integrated into the protein structure. For tetracysteine and hexahistidine motifs, dye degradation is expected to have minimal effect on the binding properties between the dye and peptide since the chromophore is indirectly bound to the protein either through arsenic-sulfur or zinc/nickel-histidine bonds. Accordingly, there would be no thermodynamic benefit in replacing a spent chromophore, so replacement with a fresh dye would be dictated by the exchange kinetics for the respective bonding interactions. The same argument could be made for the quencher-dye technology: if the dye undergoes photobleaching, this is unlikely to weaken the scFv-quencher interaction. In our fluoromodules, where the protein and dye are expected to be in intimate contact in order to provide the conformational constraints needed to enhance the dye fluorescence, the structure of a photobleached dye, which for cyanines often involves oxidative cleavage of the methine bridge,[15,31] is likely to have lower affinity than the unbleached dye, providing a thermodynamic driving force for release from the protein and replacement by a pristine dye. The low inherent fluorescence of our dyes allows an excess of the dye to be used, provided the dye does not bind nonspecifically to other components in the medium. Thus, even in cases where dye photobleaching occurs, the fluorescence can be maintained at a high level through exchange with unbleached dye from the medium, as we demonstrated for DIR in Figure 6. This is particularly useful for dyes like TO and its fluorinated derivatives, which photobleach >100-fold more efficiently than DIR and α-CN-DIR. (Compare Figures 3 and 10; note that the x-axis in these figures presents the data in terms of the number of photons absorbed per dye molecule, so the results are comparable.)

Assuming that FAPs can be expressed for intracellular applications, the key issues to address will be that the dyes (1) can be efficiently delivered into cells, (2) are nontoxic to the cells and

(3) do not bind nonselectively to cellular components at the higher concentrations needed to provide a pool of unbleached dye. Given that yeast cells can proliferate in the presence of excess TO- or MG-based dyes (some at 0.5 μM),[7] it is reasonable to anticipate that moderate concentrations of properly designed dyes will not pose significant toxicity. The higher photostability of the dyes reported here, particularly α-CN-DIR, will benefit these efforts by allowing even lower dye concentrations to be used, particularly in light of the low nanomolar K_d values for binding to K7.

CONCLUSION

The results reported here demonstrate how a promiscuous cyanine dye-binding FAP can be exploited to create new fluoromodules with improved properties: combining the protein with modified dyes that exhibit improved photostability should allow longer imaging times to be used, improving detection of low abundance or even single-molecule target proteins tagged with an scFv fluoromodule.

MATERIALS AND METHODS

Reagents for the synthesis of α-CN-DIR were purchased from Alfa Aesar or Sigma Aldrich and used without further purification. Solvents were HPLC grade. TO, TO-1F, TO-2F, TO-4F, TO-CF_3, and DIR were prepared by Dr. Gloria Silva as reported earlier.[11] 4-methyl-3-sulfopropenyl-quinolinium **(4)** was synthesized as previously reported.[11] Expression of scFv K7 on the surface of yeast and in soluble form from *E. coli* was described previously.[8]

Absorbance spectra were measured on a Cary 300 Bio UV-Visible Spectrophotometer, and fluorescence spectra were measured on a Cary Eclipse Fluorescence Spectrophotometer. DIR was excited at 580 nm, and αCN-DIR was excited at 520 nm. ^{1}H-NMR spectra were recorded on a Bruker Avance™ 300MHz instrument.

Synthesis of α-CN-DIR

2-(1,3,3-trimethylindolin-2-ylidene)acetonitrile (2)—4.06 g (0.05 moles) of sodium thiocyanate was dissolved in 50 mL of dry acetone. 6 mL (0.05 moles) of benzoyl chloride was added dropwise and then the solution was refluxed for 30 min. After cooling to room temperature, 8.66 g (0.05 moles) of 1,3,3-trimethyl-2-methyleneindole (**1**) was added dropwise and the whole brought to reflux for 30 min. The reaction mixture was diluted with acetone (50 mL) and filtered to remove the precipitate and then concentrated to give a red solid. 125 mL of dry methanol was added to dissolve the solids and then 24.38 g of a 25–30% solution of sodium methoxide in methanol was added dropwise. The solution was brought to reflux for 2 h. The solvent was removed and the resulting oil was portioned between water and methylene chloride (50/50, 200 mL). The organic layer was washed once with water, dried with $MgSO_4$, and then the solvents were evaporated. The resulting oil was put in the freezer where it solidified overnight. Residual liquid was removed by filtration and the remaining solid washed with cold methanol to give 2.5g of **2**. The yield was 25% for the two steps. ^{1}H NMR (DMSO-d_6, 300 MHz) δ: 7.32 (1H, d, J=8 Hz); 7.22 (1H, t, J=8 Hz); 6.95 (2H, t, J=8 Hz); 4.48 (1H, s); 3.14 (3H, s); 1.56 (6H, s).

2-formyl-2-(1,3,3-trimethylindolin-2-ylidene)acetonitrile (3)—0.47 g (0.005 moles) of phosphorous oxychloride was added dropwise to 0.62 mL (0.005 moles) of methyl formanilide chilled in an ice bath. After the addition was complete the solution was allowed to warm to room temperature. Complete solidification was typically observed. The solids were dissolved in 1,2-dichlorobenzene using sonication and then cooled in an ice bath. 1.0 g (0.005 moles) of **1** was added in portions (1/10th total mass) and then allowed to warm to room temperature. The solution was stirred for 24 h. The slurry was poured onto ice and made basic

with 1N NaOH. The biphasic solution was then heated to remove the organic solvent until equal portions of each layer remained, at which point the solution was allowed to cool. The upper red oil solidified allowing for the removal of the lower aqueous layer by decanting. The solid was then recrystallized from ethanol to give 0.55 g (48% yield) of **3**. ^{1}H NMR ($CDCl_3$, 300 MHz) δ: 9.73 (1H, s); 7.25–7.42 (3H, M, aromatics); 7.09 (1H, d, J=8 Hz); 3.75 (3H, s); 1.73 (6H, s).

α-CN-DIR—25 mg (1.1 mmole) of **3** and 26.5 mg (1.0 mmole) of **4** were heated to 210°C for 1 h and then allowed to cool. Column chromatographic purification using 50/50 ethyl acetate/MeOH eluted the bright pink dye in high purity (>95%) as determined by HPLC in 46% yield (21.8 mg, green solid). ε (534nm) = 81,600 M^{-1} cm^{-1} in methanol). ^{1}H NMR (CD_3CN, 500 MHz) δ: 8.94 (1H, d, J=6.5 Hz); 8.58 (1H, d, J = 8.5); 8.46 (1H, d, 9Hz); 8.23 (1H, d, 15Hz); 8.13 (1H, t, 7Hz); 7.99 (1H, d, 6.5Hz); 7.90 (1H, t, 7.5Hz); 7.44 (1H, d, 7Hz); 7.40 (1H, d, 15Hz); 7.39 (1H, d, 7.5Hz); 7.23 (1H, t, 7.5Hz); 7.17 (1H, d, 8Hz); 5.11 (2H, t, 7Hz); 3.83 (3H, s); 2.66 (2H, t, 6.5Hz); 2.39 (2H, quint, 6.5Hz); 1.75 (6H, s). ESI-MS (positive) *m/z* 473.17, calculated for $C_{27}H_{27}N_3O_3S$ *m/z* 473.17.

Fluorescence Quantum Yields

Fluorescein and Lucifer Yellow were chosen as the standards for quantum yield measurements because of the spectral overlap with the dyes under investigation. The absolute quantum yield measurements were done with the dye in the presence of free (i.e in solution, rather than at the yeast surface) protein (TO, TO-1F, TO-2F, TO-4F, TO-CF_3) or in 90% glycerol in water (α-CN-DIR). Other quantum yields were determined relative to these values. Generally, fully corrected fluorescence spectra of dye solutions having absorbance ranging from 0.02 to 0.1 (at λ_{max}) were obtained on a Photon Technologies International fluorimeter with the temperature set at 20°C. The fluorescence spectrum of each solution was integrated using Origin 6.1 and plotted against its absorbance to which a regression line of slope M was fit. The following equation was used to determine the quantum yield φ_x:

$$\Phi_x = \Phi_{sd}\left(\frac{M_x}{M_{sd}}\right)\left(\frac{\eta_x}{\eta_{sd}}\right)^2$$

where φ_{sd} is the quantum yield of the standard dye under the given conditions, M_{sd} and M_x are the slopes from the plot described above for the standard and dye respectively and η_{sd} and η_x are the refractive indices of the standard and dye solution/solvent. Refractive indices for water (buffer), 0.1 NaOH, and 90% glycerol-in-water are 1.333, 1.334, and 1.458 respectively.

Relative quantum yields were found for DIR and α-CN-DIR in the presence of K7 compared to their respective absolute quantum yields in 90% glycerol. Three solutions of dye in 90% glycerol and with K7 in buffer were made having fully corrected, absorbance-normalized fluorescence spectra with standard deviations less than ten percent. The average of the three measurements replaced M in the equation above.

Determination of K_d Values

For yeast surface-displayed scFvs, 10^7 yeast cells in wash buffer were added to dye over a selected concentration range. Fluorescence was measured using a Tecan Safire^2 96-well plate reader. The data were fit to a one-site binding equation in Origin 6.0 software, where x = the dye concentration:

$$y = \mathrm{Bmax}^{*}x/(K_d + x)$$

For the soluble protein, dye was titrated into a 10 nM K7 solution. Fluorescence was recorded on a Photon Technologies International fluorimeter, and was fit to the same equation.

Photobleaching

Direct Irradiation—Since some of the dyes were bleached under different excitation filters it was necessary to quantify the number of photons each dye solution was receiving. The dyes were excited using a Zeiss Axiovert 200 equipped with a mercury arc lamp (HBO 100) using a 20×0.75 NA Plan Achromat objective. Chroma filter set #41017 composed of HQ470/40x, Q495LP(reflector), and HQ525/50m filters was used for TO, TO-1F, TO-2F, TO-4F and TO-CF_3. Chroma set #31002 consisting of D540/25x, 565 DCLP(reflector), and D605/55m was used for α-CN-DIR. The filter set for DIR was D595/40x, Q660LP(reflector), and HQ700/75m, the last two being from Chroma set #41008. To determine the effective extinction coefficient (ε_{eff}, needed to quantify the number of photons the dyes were receiving) an 818 SL silicon photodiode connected to a Newport 1815C Power Meter was placed in the excitation pathway. Glass capillaries with a thickness of 0.2 mm (dx) were filled with 100 μM dye solution in buffer or 90% glycerol and then sealed and fixed to a clean slide. Power readings were taken on these solutions to give **P** as well as on respective blank solutions to give $\mathbf{P_0}$. Solving the following equation for ε_{eff} allows us to normalize all of the dye solutions such that the rate of excitation would be constant at the beginning of each experiment.

$$A=\log(P_0/P)=\varepsilon_{eff}\times[\mathrm{Dye}]\times dx$$

Solutions of dye with protein and in 90% glycerol were made with concentrations ranging from 0.1μM to 0.569 μM based on the above calculations. A Hamamatsu ORCA-ER CCD camera 1280 × 1024 with 6.45 μM square CCD elements was used to capture the fluorescence images of these solutions using the filter sets described above. For TO, TO-1F, TO-2F, TO-4F, TO-CF_3 bleaching was observed over ten seconds (continual irradiation) while taking four imagles per second. For DIR and α-CN-DIR bleaching was observed over 40 seconds, taking one image per second. Experiments over 40 seconds were not conducted because dye diffusion into or out of the excited area begins to affect the measurements. Each trial was performed in triplicate. QED In Vivo software was used to control the microscope, camera and excitation. ImageJ software was used to create time series of the image sequences from 500 × 500 pixel areas and subsequent quantification of fluorescence as a function of image number.

To quantitatively compare the photobleaching of DIR and TO dyes in this study, we plotted all time series data versus mean number of photons absorbed per dye molecule. To obtain the correct scale factor, the excitation intensity (I_0) and effective extinction coefficient (ε_{eff}) was determined for the specific dye and filter set combinations used. In all cases, power (P) was measured directly, and intensity computed as power divided by the area of the microscope illuminated field-of-view ($S = \pi r^2$). I_0 was computed from a measurement of total power (P_{in}) entering the back of the microscope objective:

$$I_0=P_{in}/S=P_{in}\,\pi r2 \quad (1)$$

Typically, P_{in} ranged from 8–18 mW, and the field diameter was set at 600μm (area = 2.83×10^{-3} cm^2). Therefore, I_0 was typically 4.5 W/cm^2, roughly 700 times greater than direct sunlight in a comparable wavelength band. Using a 100μM dye test solution in a 0.02cm path-length flat capillary tube (VitroCom #3520), incident power (P_o) and exiting power (P) were measured using a photodiode laser power meter calibrated in mW (Newport 1815-C, 818-SL diode) for all initial determinations of light absorption in the microscope setup.

Because we utilized fixed bandpass filters that matched to varying degree the absorption bands of the dyes tested, the monochromatic Beer-Lambert law does not apply directly. For this narrow-band, but polychromatic case, the effective extinction coefficient was defined by the modified Beer-Lambert relation:

$$\varepsilon_{\text{eff}} \text{C L} = \log(\text{P}_\text{o}/\text{P}) \tag{2}$$

where C = dye molar concentration, L = path length (0.02cm), and P is the transmitted polychromatic power. It can be shown that ε_{eff} is related to the monochromatic extinction coefficient by:

$$\varepsilon_{\text{eff}} = \int s(\lambda)\, \varepsilon\, (\lambda)\, \text{d}\lambda \tag{3}$$

where s(λ) is the normalized incident light spectrum produced by the microscope lamp and filter combination.

The excitation rate per dye molecule (R′) in dilute test samples was then computed from the linearized Beer-Lambert relation, the mean photon energy for the bandpass filter in use (E = hc/λ), and the number of dye molecules in the field of view (N_{dye}):

$$\text{R}' = (\Delta \text{P}/E)/\text{N}_{\text{dye}} \tag{4}$$

where ΔP is:

$$\Delta \text{P} = \text{P}_\text{o}(1 - 10^{-\text{A}}) \approx \text{P}_\text{o}(\ln 10)\varepsilon_{\text{eff}}\, \text{C L} \tag{5}$$

Using equation (1), (4), and (5) we obtain:

$$\text{R}' = 2303\, \lambda\, \varepsilon_{\text{eff}}\, \text{I}_0/hc\text{N}_{\text{avo}} \tag{6}$$

which has units of photons absorbed per second per dye molecule, and, as expected, is independent of dye concentration. Experimentally, I_0 was determined from P_{in} and S, and ε_{eff} was determined from P_0, P, C, and L in a separate measurement. The appropriate R′ was then used to scale the time base of each photobleaching run, and the results plotted in Figures 3 and 9.

To demonstrate fluoromodule regeneration, samples containing 250 nM DIR and K7 were irradiated with a 150 watt Xe lamp using an Oriel lamp house (model #6602) equipped with a water filter (Oriel #6117) and powered by an Oriel 68805 universal power supply (40–200 watts). The white light was passed through a 455 nm glass longpass filter. Samples were immersed in an 18±2°C water bath during irradiation periods. Fluorescence was recorded before and after 15 minutes irradiation. An additional equivalent of DIR (250 nM) was then added to the irradiated sample and the fluorescence spectrum was recorded. The same experimental setup was used to compare H_2O and D_2O for direct photobleaching of the dye-protein complexes.

Thermal Bleaching

Bleaching experiments in the presence of 50 mM sodium molybdate and 9 mM hydrogen peroxide contained 1 uM of dye with or without 1 uM K7 protein. The buffer solutions were adjusted so that the final ionic strength would be the same as the standard wash buffer with pH=9.0. 10% H_2O_2 was added to the buffer solution to give a final concentration of 9.8 mM. The absorbance and fluorescence spectra of the dye and protein in the buffer solution were recorded and then Na_2MoO_4 was added to the solution. Scans were taken at 10 minute intervals over a total of 40 minutes.

Fluorescence Microscopy

Confocal fluorescence and transmitted light DIC images were recorded on a Carl Zeiss LSM 510 Meta confocal microscope for yeast surface-displayed K7 and various dyes. TO dyes were excited using the 488 nm line of an argon ion laser with a 505–550 nm band pass filter for detection with a photomultiplier tube. DIR dyes were excited with a 561 nm solid state diode laser with a 575–630 nm band-pass filter for detection with a photomultiplier tube. Dye concentrations are given in caption to Figure 10; cells were stained for ca. 30 min and then imaged without washing away unbound dye.

Supplementary Material

Refer to Web version on PubMed Central for supplementary material.

Acknowledgments

NS synthesized α-CN-DIR and performed spectroscopic experiments with this dye. KZ performed spectroscopic experiments with fluorinated TO dyes. DIR and fluorinated TO dyes were synthesized by Dr. Gloria Silva. We thank Dr. James Fitzpatrick for fluorescence microscope images. NMR spectra were recorded in the CMU NMR facility, supported by NSF grant CHE-0130903. We are grateful to Hayriye Özhalici-Ünal for supplying soluble K7 protein and for helpful discussions. This work was supported by the NIH (U54 RR022241). NS and KZ gratefully acknowledge support from ARCS and NDSEG Graduate Fellowships, respectively.

References

1. Morise H, Shimomura O, Johnson FH, Winant J. Biochemistry 1974;13:2656–2662. [PubMed: 4151620]
2. Shimomura O, Johnson FH, Saiga Y. J Cell Comp Physiol 1962;59:223–239. [PubMed: 13911999]
3. Chalfie M, Tu Y, Euskirchen G, Ward WW, Prasher DC. Science 1994;263:802–805. [PubMed: 8303295]
4. Inouye S, Tsuji FI. FEBS Lett 1994;341:277–280. [PubMed: 8137953]
5. Tsien RY. Annu Rev Biochem 1998;67:509–544. [PubMed: 9759496]
6. Ward, TH.; Lippincott-Schwartz, J. Green Fluorescent Protein. Vol. 2. Chalfie, M.; Kain, SR., editors. John Wiley & Sons; Hoboken, NJ: 2006. p. 305-337.
7. Szent-Gyorgyi C, Schmidt BF, Creeger Y, Fisher GW, Zakel KL, Adler S, Fitzpatrick JA, Woolford CA, Yan Q, Vasilev KV, Berget PB, Bruchez MP, Jarvik JW, Waggoner A. Nature Biotechnol 2007;26:235–240. [PubMed: 18157118]
8. Özhalici-Ünal H, Lee Pow C, Marks SA, Jesper LD, Silva GL, Shank NI, Jones EW, Burnette JM III, Berget PB, Armitage BA. J Am Chem Soc 2008;130:12620–12621. [PubMed: 18761447]
9. Constantin T, Silva GL, Robertson KL, Hamilton TP, Fague KM, Waggoner AS, Armitage BA. Org Lett 2008;10:1561–1564. [PubMed: 18338898]
10. Renikuntla BR, Rose HC, Eldo J, Waggoner AS, Armitage BA. Org Lett 2004;6:909–912. [PubMed: 15012062]
11. Silva GL, Ediz V, Armitage BA, Yaron D. J Am Chem Soc 2007;129:5710–5718. [PubMed: 17411048]

12. Sun WC, Gee KR, Klaubert DH, Haugland RP. J Org Chem 1997;62:6469–6475.
13. Spagnuolo CCVRJ, Jares-Erijman EA. J Am Chem Soc 2006;128:12040–12041. [PubMed: 16967933]
14. Sun W, Gee KR, Haugland RP. Bioorg Med Chem Lett 1998;8:3107–3110. [PubMed: 9873685]
15. Toutchkine A, Nguyen DV, Hahn KM. Org Lett 2007;9:2775–2777. [PubMed: 17583344]
16. Coenen M, Weissel O. ω-Aldehydes of N-substituted ω-Cyano-Methylene Indoline Derivatives. Oct. 18;1960 US 2957005
17. Debler EW, Kaufmann GF, Meijler MM, Heine A, Mee JM, Pljevaljcic G, Di Bilio AJ, Schultz PG, Millar DP, Janda KD, Wilson IA, Gray HB, Lerner RA. Science 2008;319:1232–1235. [PubMed: 18309081]
18. Aubry JM. J Am Chem Soc 1985;107:5844–5849.
19. Böhme K, Brauer HD. Inorg Chem 1992;31:3468–3471.
20. Hayashi Y, Shioi S, Togami M, Sakan T. Chem Lett 1973:651–654.
21. Merkel PB, Kearns DR. J Am Chem Soc 1972;94:7244–7253.
22. Matheson BC, Etheridge RD, Kratowich NR, Lee J. Photochem Photobiol 1975;21:165–171. [PubMed: 1169776]
23. Miesenbock G, De Angelis DA, Rothman JE. Nature 1998;394:192–5. [PubMed: 9671304]
24. Adams SR, Campbell RE, Gross LA, Martin BR, Walkup GK, Yao Y, Llopis J, Tsien RY. J Am Chem Soc 2002;124:6063–6076. [PubMed: 12022841]
25. Hauser CT, Tsien RY. Proc Natl Acad Sci USA 2007;104:3693–7. [PubMed: 17360414]
26. Rozinov MN, Nolan GP. Chem Biol 1998;5:713–28. [PubMed: 9862799]
27. Marks KM, Rosinov MN, Nolan GP. Chem Biol 2004;11:347–356. [PubMed: 15123264]
28. Farinas J, Verkman AS. J Biol Chem 1999;274:7603–6. [PubMed: 10075643]
29. Sparano BA, Koide K. J Am Chem Soc 2005;127:14954–14955. [PubMed: 16248596]
30. Sparano BA, Koide K. J Am Chem Soc 2007;129:4785–4794. [PubMed: 17385867]
31. Byers GW, Gross S, Henrichs PM. Photochem Photobiol 1978;23:37–43. [PubMed: 1265127]

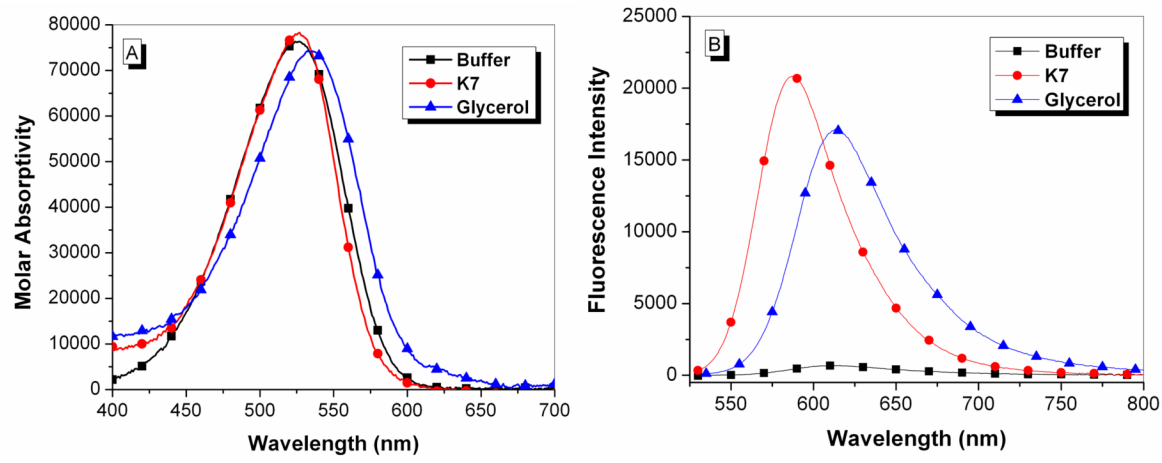

Figure 1.

UV-vis absorption (A) and fluorescence emission spectra (B) recorded for 0.6 μM α-CN-DIR in aqueous buffer (squares), 90% glycerol-in-water (triangles) and FAP K7 (circles). Samples in (B) were excited at 520 nm.

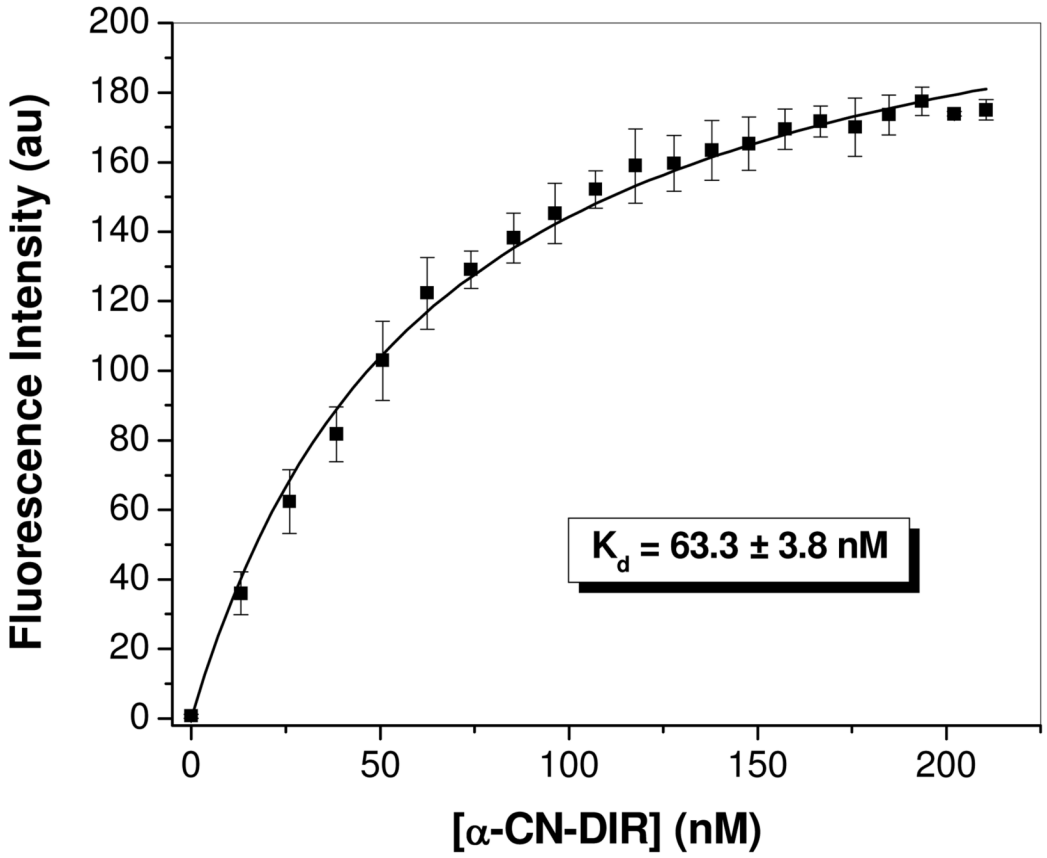

Figure 2.
Binding of α-CN-DIR to scFv K7 as shown by fluorescence titration. Samples contained 10 nM [K7] and were excited at 534 nm. Solid line is fit to a 1:1 binding model.

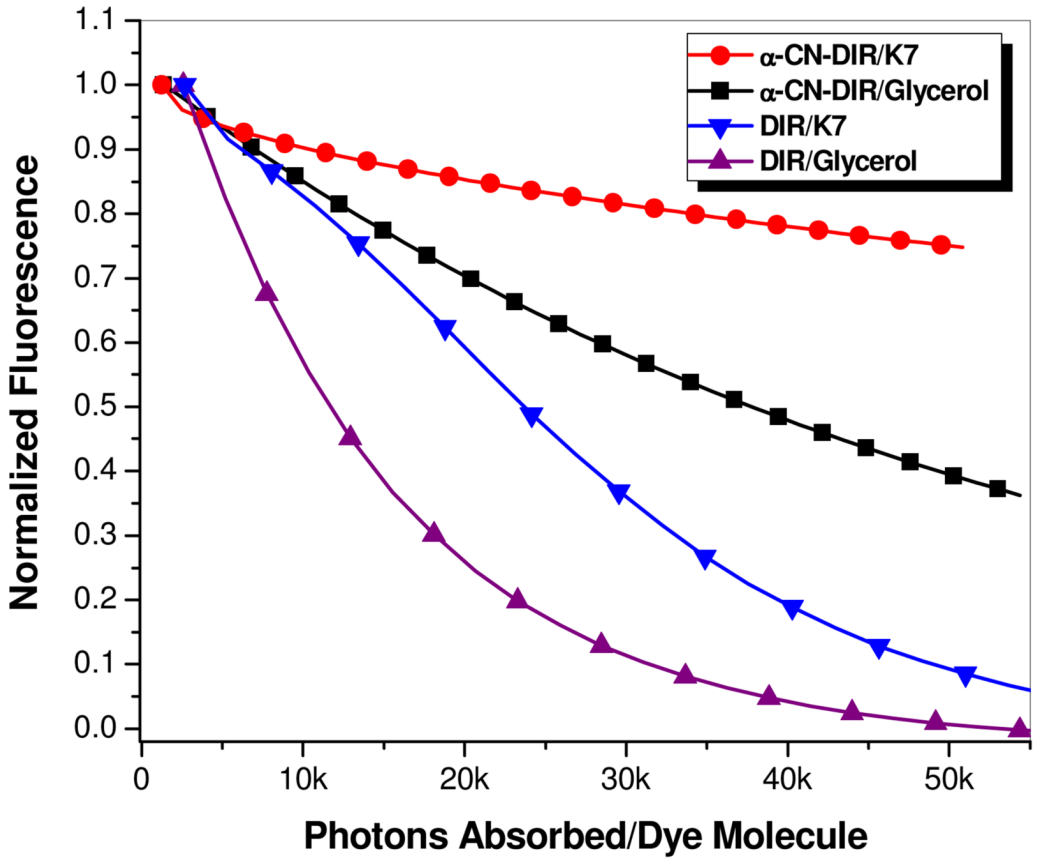

Figure 3.
Photobleaching of DIR and α-CN-DIR in 90% glycerol or in the presence of scFv K7. Samples were excited at 595 ± 20 nm (DIR) and 540 ± 12.5 nm (α-CN-DIR). Concentrations were adjusted to ensure initial equivalent absorbances at the excitation wavelength.

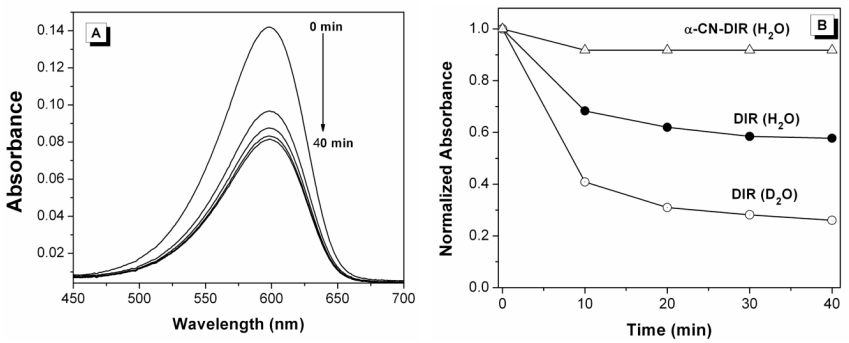

Figure 4.

Reaction of DIR and α-CN-DIR with singlet oxygen produced by sodium molybdate and H_2O_2. Reactions were run in water with [Dye] = 1 μM and pH = 9. [Na_2MoO_4] = 50 mM, [H_2O_2] = 9.8 mM. (A) DIR absorbance spectra recorded in H_2O during reaction with Na_2MoO_4 and H_2O_2. (B) Time course for dye bleaching for DIR in H_2O and D_2O as well as α-CN-DIR in H_2O.

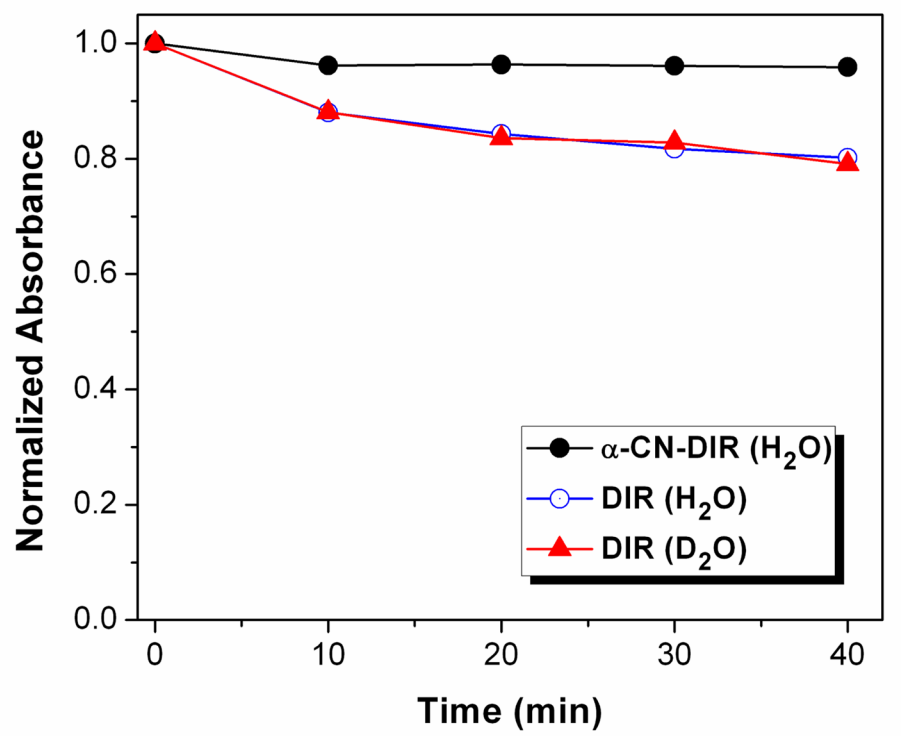

Figure 5.
Reaction of K7-bound DIR and α-CN-DIR with singlet oxygen produced by sodium molybdate and H_2O_2. Reactions were run in buffer with [Dye] = [K7] = 1 μM and pH = 9. [Na_2MoO_4] = 50 mM, [H_2O_2] = 9.8 mM.

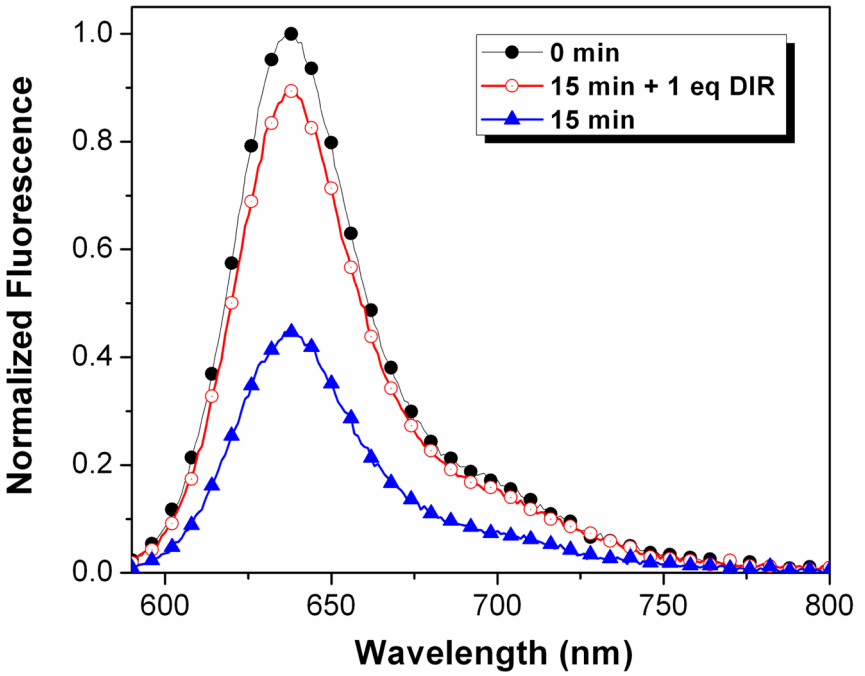

Figure 6.

Photobleaching of DIR/K7 by direct irradiation at λ > 455 nm for 15 min. Initial [DIR] = [K7] = 250 nM. Fluorescence emission spectra (λ_{ex} = 590 nm) were recorded before and after 15 min irradiation. After irradiation, one equivalent of fresh DIR was added to the cuvette and the fluorescence spectrum was recorded.

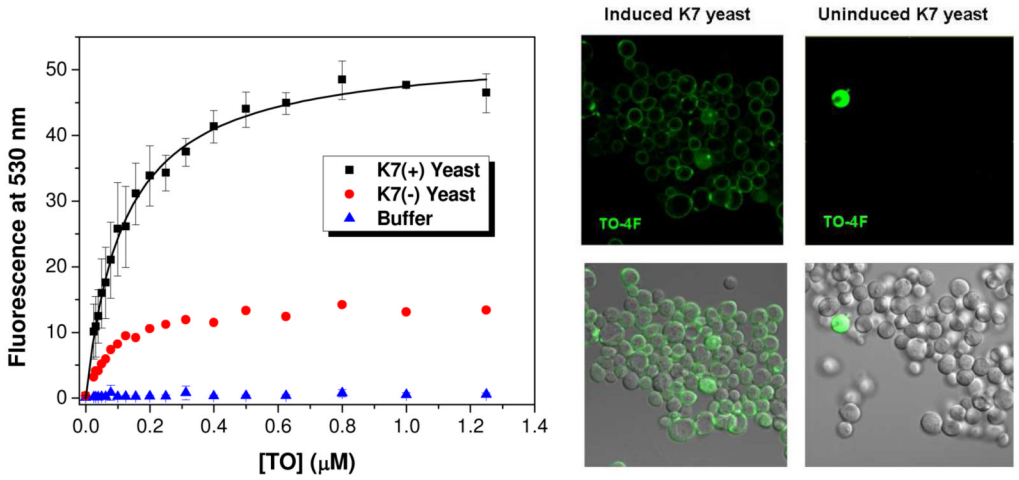

Figure 7.

(Left) Fluorescence titration of TO into yeast-surface displayed K7. Line is fit to a 1:1 binding model. Dye was titrated into yeast cells expressing K7 (squares), yeast not expressing K7 (circles), and buffer (triangles). Samples were excited at 480 nm. (Right) Confocal fluorescence microscope images of yeast stained with 300 nM TO-4F either with or without inducing expression of the surface-displayed K7 protein. Samples were excited at 488 nm and fluorescence was collected at 517–583 nm. Bottom panels show merge of fluorescence and differential interference contrast images.

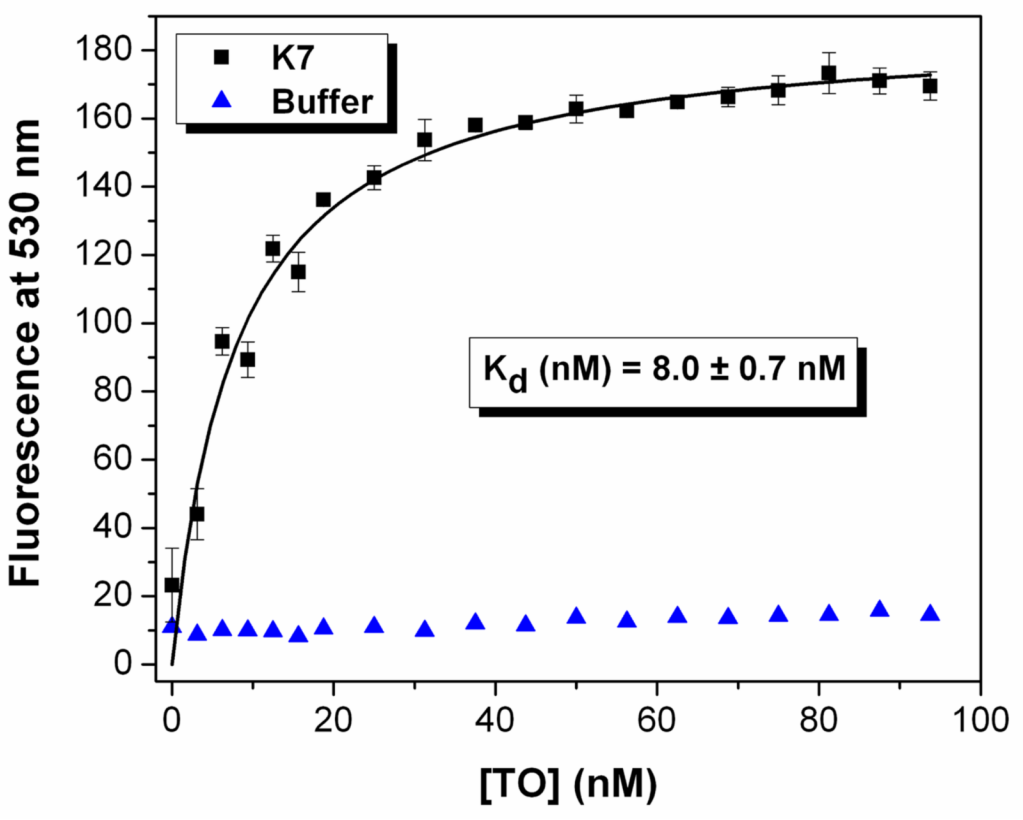

Figure 8.
Fluorescence titration of TO into soluble K7. Dye was titrated into 10 nM soluble K7 (squares) and buffer (triangles). Data were fit to a 1:1 binding model (solid line). Samples were excited at 480 nm.

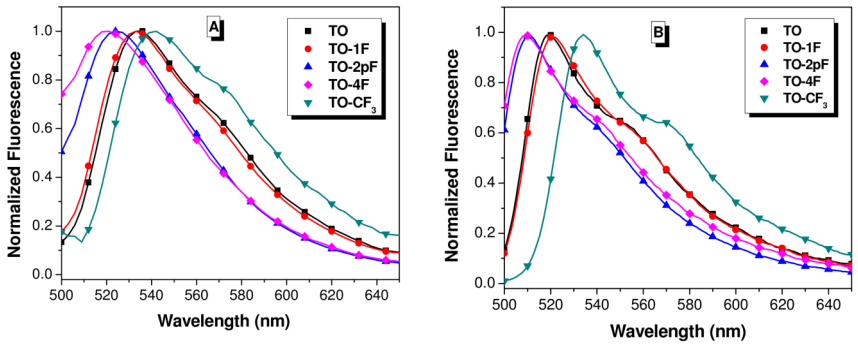

Figure 9.

Fluorescence spectra of TO and fluorinated analogues bound to K7 protein displayed on the surface of yeast (A) or in solution (B). [Dye] = 300 nM in both cases. For (A), 10^7 cells used. For (B), 600 nM soluble K7 used. Samples were excited at 480 nm.

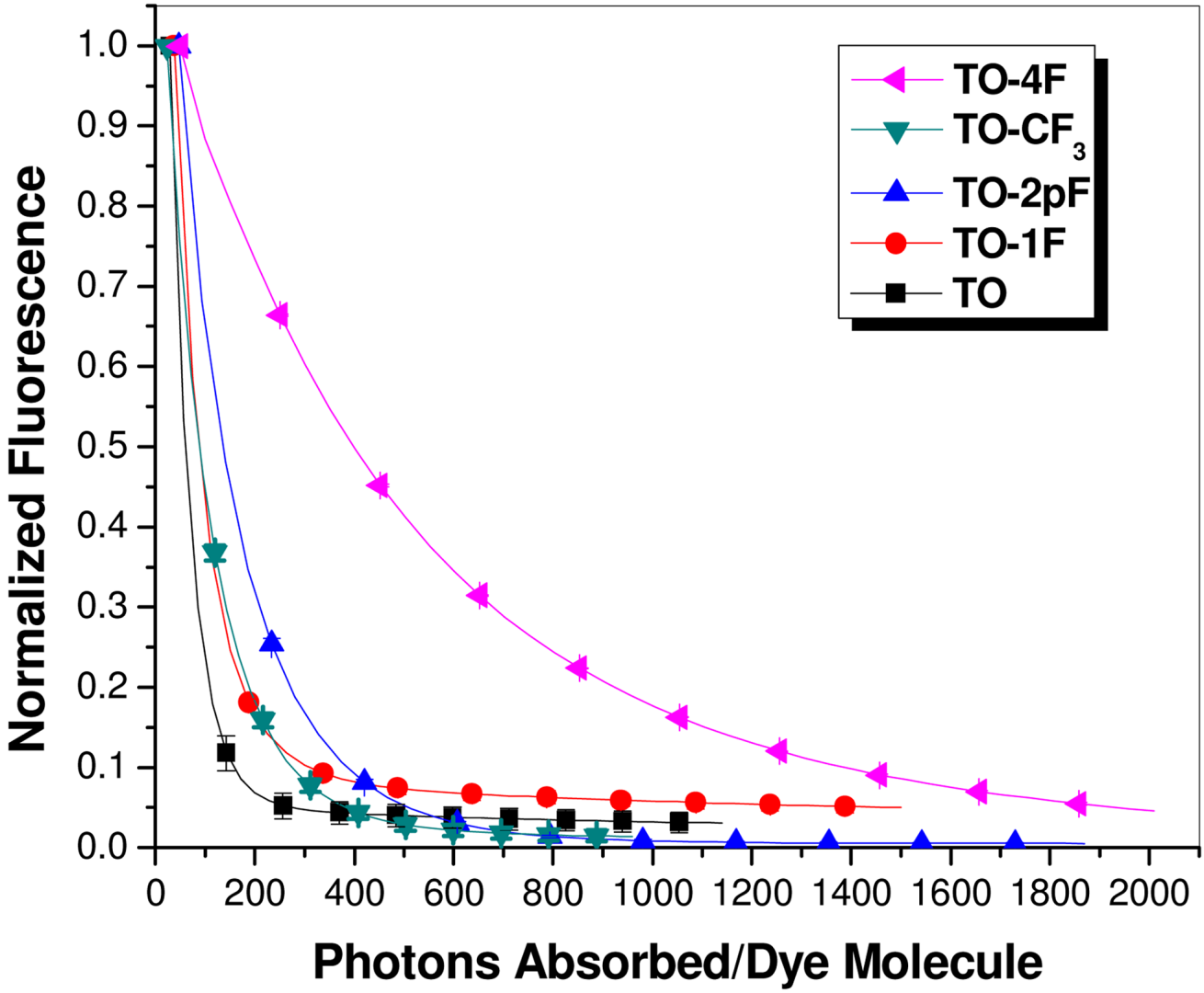

Figure 10.
Photobleaching of TO dyes with soluble K7. Concentrations were adjusted to give equivalent absorbances at the excitation wavelength (470 ± 20 nm).

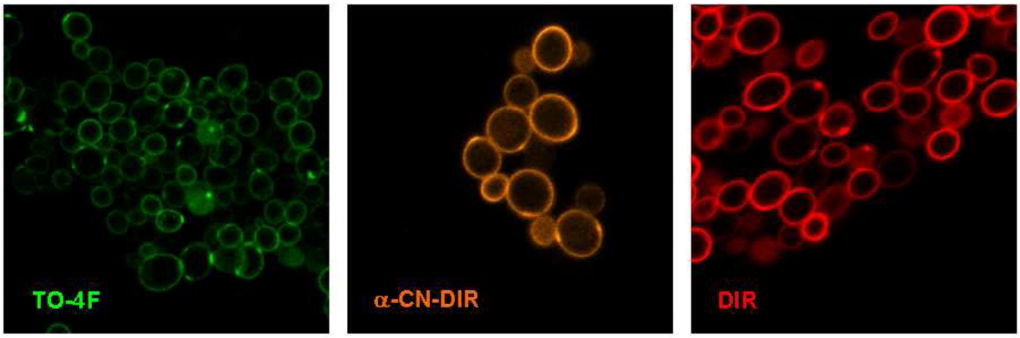

Figure 11.
Confocal fluorescence micrographs of yeast-displayed scFv K7 stained with 300 nM TO-4F (left), 200 nM α-CN-DIR (middle) and 100 nM DIR (red). (Fluorescence and differential interference contrast overlay images are shown in supporting information, Figure S3.)

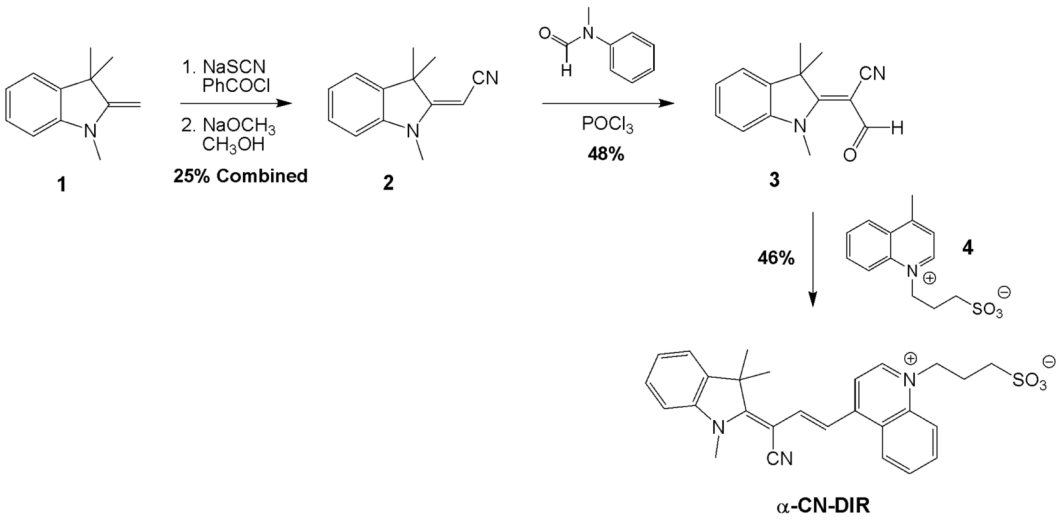

Scheme 1.

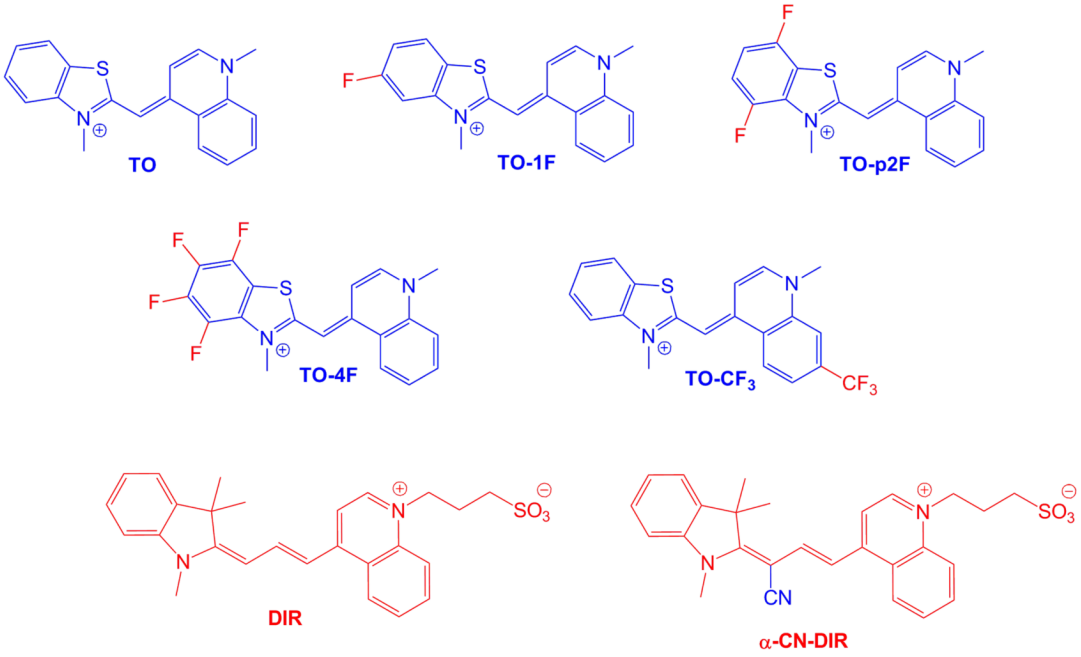

Chart 1.
Fluorogenic cyanine dyes based on thiazole orange (TO) and dimethylindole red (DIR) chromophores.

Table 1

Fluorescence quantum yields (φ_f) and equilibrium dissociation constants (K_d) for fluorogenic cyanine dyes bound to scFv K7. φ_f values in 90% glycerol-in-water shown for comparison.

Dye	φ_f (Glycerol)	φ_f (K7)	K_d (nM) Soluble K7	K_d (nM) Yeast-Displayed K7
DIR	0.15[a]	0.33	10.3 ± 0.7	13.9 ± 3.2
α-CN-DIR	0.19	0.18	63.3 ± 3.8	41.9 ± 1.9
TO	0.027[b]	0.17	8.0 ± 0.7	119 ± 5.5
TO-1F	0.029[b]	0.25	7.1 ± 0.9	52.7 ± 7.8
TO-2pF	0.038[b]	0.30	9.6 ± 0.6	88.3 ± 14.5
TO-4F	0.051[b]	0.26	4.0 ± 0.4	18.7 ± 3.4
TO-CF_3	0.017[b]	0.14	19.5 ± 1.1	12.8 ± 2.0

[a] Reference 3;

[b] Reference 15